J.nr.: SICAM.01.05.011

Self-oscillating modulators for direct energy conversion audio power amplifiers

Petar Ljušev[1], Michael A.E. Andersen[1]

[1]*Ørsted • DTU Automation, Technical University of Denmark, Kgs. Lyngby, DK-2800, Denmark*

Correspondence should be addressed to Petar Ljušev (pl@oersted.dtu.dk)

ABSTRACT

Direct energy conversion audio power amplifier represents total integration of switching-mode power supply and Class D audio power amplifier into one compact stage, achieving high efficiency, high level of integration, low component count and eventually low cost. This paper presents how self-oscillating modulators can be used with the direct switching-mode audio power amplifier to improve its performance by providing fast hysteretic control with high power supply rejection ratio, open-loop stability and high bandwidth. Its operation is thoroughly analyzed and simulated waveforms of a prototype amplifier are presented.

1. INTRODUCTION

The switching-mode power conversion technology has radically changed the today's commercial product appearance, making them far smaller than few decades ago and leaving the designers bare hands to experiment with their look and feel without being limited by technology barriers. These benefits are direct result of the improved efficiency of the power supplies and power amplifiers that use switching approach instead of the linear one. As a side effect, the amount of heat-sinking material needed is reduced by at least an order of magnitude, which improves the level of integration between the various control and power components, so that the overall board space, weight and volume are significantly reduced and power density is improved. The aforementioned advantages are probably most clearly seen in the switching-mode Class D audio power amplifiers, where the new efficient power conversion principle has opened the doors to some new and challenging application areas, from the smallest low-end portable devices with extended battery life to the large high-end audio installations for stage performances with tremendously reduced dimensions.

The achievements in the field of switching-mode audio power amplification in the last few years, described in terms of even higher output power levels and improved audio performance, are drawing this approach on the technology map as one of the most significant breakthroughs that is eventually going to replace linear electronics in most of the power processing applications. However, this does not mean that the present Class D audio power amplifiers are the only possible solution that fits all applications, and much research is done in order to take the most advantage from the very high conversion efficiency of the switching-mode approach while still keeping the complexity and component count to minimum. These unique challenges, posed predominantly by the audio and video product manufacturers wanting to penetrate the low-end market by cutting production costs and introducing cheap products of satisfactory quality, can be answered by further and closer integration of the constitutive parts of the audio power amplifier - the switching-mode power supply and the Class D amplifier, which have been till know usually viewed as separate parts without many touching points. This integration philosophy leads to a very compact audio power amplification solution known as "SIngle Conversion stage AMplifier" or SICAM [1], [2], [3], [4], meaning that the new audio power amplifier is capable of direct energy conversion from the AC mains to the loudspeaker output. It is therefore very interesting for the Active pulse modulated Transducer (AT) [5] intended for use in the new generation of active loudspeaker systems and subwoofer units.

This paper will introduce a new control approach for SICAMs, that utilizes self-oscillating principle to improve the performance of present SICAM solutions [2], [6], [7]. The operation principles of the self-oscillating modulator for SICAM are thoroughly analyzed, together with the SICAM topology that is considered as the most suitable for the purpose. At the end, experimental results are shown that prove the feasibility of the approach.

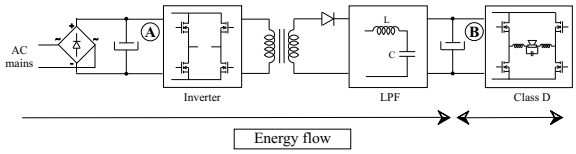

Fig. 1: Conventional Class D audio power amplifier

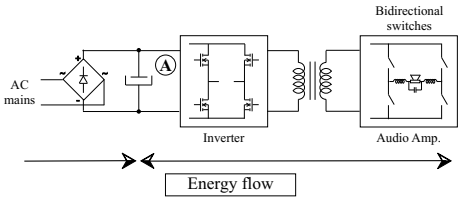

Fig. 2: Direct conversion audio power amplifier

2. AUDIO AMPLIFICATION WITH SICAM

The block diagram of the conventional Class D audio power amplifier is given in Fig. 1. It can be principally divided into two parts: switching-mode power supply (SMPS) and Class D audio power amplifier. The simplified front-end SMPS consists of mains rectifier, energy buffering capacitor A, high frequency (HF)-operated inverter stage, small power transformer, output rectifier and low-pass filter (LPF) with a bulky capacitor B, which keeps the voltage of the associated DC-bus to a constant value. Heavy filtered DC-bus is used to connect the SMPS with the Class D audio power amplifier, consisting from simple power switches in half- or full-bridge configuration and low-pass output filter. It can be noticed that this conventional solution incorporates two bulky energy storage capacitors A i B, where the former is used to overcome the physical constraint of the mains voltage regular zero-crossings and is therefore compulsory, while the latter is required by the specific topology used and can be possibly avoided by using some other energy conversion approach. As another drawback, the energy direction is kept unidirectional through the whole SMPS, so that any charge returned back from the Class D amplifier accumulates in the B capacitors and causes perturbations on the DC-bus voltage that can lead to power supply pumping problems with single-ended Class D amplifiers reproducing low frequency (LF) signals.

The block diagram of the direct energy conversion audio power amplifier or SICAM is presented in Fig. 2. It is developed from the HF-link power converter topology [8] which is being proposed for use in Uninterruptible Power Supplies (UPS) and converters for renewables where isolation is mandatory. The main feature is the replacement of the SMPS DC-bus with a HF-link, i.e. the isolation transformer is used as a connection point between the simplified power supply and the audio power amplifier, now comprising of bidirectional switches which are capable of blocking both voltage polarities and conducting current in both directions. In this way, the whole power conversion chain is shrunk resulting in higher efficiency, and the bulky LPF with capacitor B in the conventional SMPS is removed together with the output rectifiers, thus allowing bidirectional output flow through the isolation barrier down to the energy storage capacitor A. Therefore, the power supply pumping problems are non-existent with the newly proposed SICAM. The biggest problem with the presented approach is the load current commutation between the bidirectional switches in the amplifier, since the freewheeling path through the MOSFET body diodes in the Class D amplifier disappears when using bidirectional switches. Through the years many different approaches have been proposed to solve the commutation problem by using special modulation techniques [3], dissipative and active clamps [4], [7] or safe-commutation switching strategies [2], [6] and some of them will be reviewed in the later sections.

In the following sections, the switching stage on the primary side of the main transformer will be referred as input stage, primary stage or inverter stage, while the one on the secondary side will be referred as output stage, secondary stage or bidirectional bridge.

3. SELF-OSCILLATING MODULATORS FOR AUDIO AMPLIFIERS

The basic approach of creating Pulse Width Modulated (PWM) output voltage has not changed from the dawn of signal processing era. Essentially, reference voltage is being compared against the triangular carrier and their intersection points define the switching instants. The performance of the modulator strongly depends on the cleanliness of the triangular carrier and any distortion of its shape leads to unpleasant nonlinear effects [9]. The sources of carrier distortion are often difficult to reveal, since they can be either result of the non-ideal external carrier generator or can appear as a side effect of the ripple present in the feedback signal from the power stage.

The most basic PWM modulators use externally generated triangular and their main advantage is the constant switching frequency operation, which makes it very easy to predict the frequency content of the output and filter it accordingly. It also features constant gain, equal to the inverse of the carrier voltage peak V_c, $K_{PWM} = 1/V_c$, which is independent of the modulation index or the modulation frequency, up to half the carrier frequency. Unfortunately, without any power supply voltage feedforward implemented, they have low Power Supply Rejection Ratio (PSRR), which is usually compensated by adding additional feedbacks from the amplifier output and providing high gains within the corresponding compensators. To decrease the carrier distortion from output voltage ripple residues in the feedback, the switching frequency is usually chosen an order of magnitude higher than the power bandwidth and output filter cut-off frequency, while the control bandwidth is intentionally limited to reasonable values, thus limiting audio performance. Turning to practical implementation, these PWM modulators require expensive high bandwidth operational amplifiers in the external carrier generator, which makes them less appealing.

PWM modulators, which do not utilize externally generated carrier are the self-oscillating modulators [10], [11], [12]. Since the self-oscillating modulator creates the carrier and hysteresis window internally using the power stage, these modulators are usually characterized with very high PSRR, good cancellation of various errors and disturbances, open-loop stability and simplicity. From control perspective, the modulator itself has the largest possible bandwidth, which is equal to the switching frequency, since that is the oscillation point where the open-loop transfer function has a gain of 1 with phase shift equal to 180°. Disturbances are, however, effectively rejected in the interval where the open-loop transfer function has substantial gain (ex. 20 dB or more). On the other hand, most of the present self-oscillating modulators have variable switching frequency with changing modulation indexes M, which causes the amplifier to experience very large voltage ripple, low control bandwidth and high distortion close to the maximum modulation index. This problem is alleviated by limiting the modulation index to a value lower than 1 (ex. $M_{max} = 0.8$) i.e. increasing the power supply voltage with respect to the maximum load voltage. Despite of the few disadvantages, self-oscillating modulators are found in most of the commercial Class D audio power amplifiers.

4. SELF-OSCILLATING MODULATORS FOR SICAMS

4.1. Application and limitations

The most common modulator for direct conversion audio power amplifiers, i.e. SICAMs [2], [3], [4], [6], [7] has up till now been the PWM modulator with externally generated carrier. Reasons for this are mainly twofold and arise from the fact that self-oscillating modulators have variable switching frequency that decreases with increasing modulation index and the inability to predict and steer switching instants, due to the hysteretic-type control. On one hand, when using self-oscillating modulators in SICAMs with PWM modulated transformer voltages [3], variable switching frequency causes the transformer design to be suboptimal and its dimensions must be chosen to bare the largest magnetic flux at lowest switching frequency without going into saturation. On the other hand, when PWM modulation is used only on the secondary side of the transformer in conjunction with some safe-commutation principle [2], the random switching of self-oscillating modulator makes it very difficult to synchronize the operation of the input stage to the output stage. However, this does not mean that self-oscillating modulators are completely useless in SICAMs, but rather that they are applicable just with certain SICAM topologies and usually with active [7] or dissipative clamps [4], or conditionally with safe-commutation strategies [2] as means for commutating the load current in the output bidirectional bridge.

In the next sections, the use of self-oscillating modulators will be analyzed with respect to SICAMs with non-modulated transformer voltages [2], where the input inverter stage on the primary side of the transformer is operated with 50% duty cycle to create rectangular transformer voltage with maximum width. The operation of the input stage is not synchronized to any control signal from the secondary side, and therefore the operation of the input stage is referred as free-running.

4.2. Operation fundamentals

Self-oscillating modulators can be roughly divided into two groups: current mode and voltage mode modulators [12]. There is not bigger difference in their principal operation, except that the measured inductor current in the former group is used directly in the modulator, while in the latter group the measured bridge voltage must be first integrated or processed in some way in the control sec-

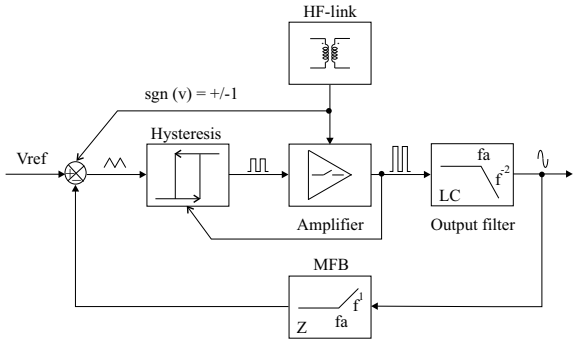

Fig. 3: GLIM for SICAM

tion [13] or in both control section and power stage [10], [14].

The approach presented in the following few paragraphs can be used to modify particular self-oscillating modulator for SICAM operation in a straightforward manner. Without loss of generality, the discussion will deal just with the Global Loop Integrating Modulator (GLIM) [14], where the integrating transfer function from the bridge voltage to the input of the hysteresis block is obtained by combining the poles of the output filter in the power stage with the zero in the modulator feedback block (MFB) at the output filter cut-off frequency. The hysteresis block itself is created from the power stage bridge voltage using a resistive divider, as an input to the comparator.

In all self-oscillating modulators, the polarity of the bridge voltage which is being applied across the output filter and loudspeaker is determined solely by the state of the comparator i.e. the output from the hysteresis block, since the power supply voltage has constant polarity. In SICAMs, bridge voltage essentially represents a product of the HF-link voltage and the state of the comparator. Changing the HF-link polarity causes immediate change in the bridge voltage and hysteresis window polarity bound to it, which will surely bring the power stage into stall due to the ill-posed hysteresis limits. Therefore, any change in the HF-link voltage polarity must be followed by corresponding change in the direction of integration, which essentially means that the polarity of the feedforward and feedback signals entering the comparator must be reversed. The block diagram of the proposed GLIM self-oscillating SICAM is given in Fig. 3.

Since the operation of the proposed self-oscillating modulator for SICAMs seems to be determined by the quantities characteristic for the basic self-oscillating modulator intended for operation with Class D amplifiers, quantities associated with the latter will be called basic quantities and will be given asterisk "*" as superscript. Notice that most of these quantities are severely affected and altered when the SICAM HF-link is included in the modulator.

The operation of the self-oscillating modulator for SICAMs depends on the modulation index M of the reference voltage signal at the input of the modulator. Let M^*_{lim} denote the modulation index limit at which the frequency of the basic self-oscillating modulator, equal to the output stage switching frequency f^*_{s2} is two times the switching frequency of the free-running input stage f_{s1}:

$$f^*_{s2}(M^*_{lim}) = 2 \cdot f_{s1} \tag{1}$$

4.3. Normal operation with $M < M^*_{lim}$

Normal operation of the self-oscillating modulator in Fig. 3, which occurs for modulation indexes $M < M^*_{lim}$ is shown in Fig. 4. The operation is called normal since it resembles very much the operation of a conventional Class D amplifier with self-oscillating modulator. With low modulation indexes $M < M^*_{lim}$, the slopes of both the raising portion and the falling portion of the carrier are steep and the output stage performs several switchings within each period of the HF-link voltage v_{HF}. The nature of the operation makes it very difficult to determine the exact switching frequency of the output stage, since it depends not only on the feedback quantities but also on the instants when HF-link changes its polarity. It can be, however, assumed that with sufficient level of accuracy the average switching frequency of the output stage f_{s2} is equal to the switching frequency of the basic self-oscillating modulator f^*_{s2}:

$$f_{s2}(M) = f^*_{s2}(M) = \frac{V_s}{4} \frac{1 - M^2}{\tau_{int} V_h + t_d V_s} \bigg|_{M<M^*_{lim}} \tag{2}$$

where $V_s = |v_{HF}|$ is the absolute value of the HF-link voltage, V_h is the hysteresis window width, t_d is the modulator loop delay and τ_{int} is the integrator time constant which is equal to the output filter cut-off frequency in the GLIM case. In all practical implementations, the hysteresis window is formed using the HF-link voltage:

$$V_h = k_h \cdot V_s \tag{3}$$

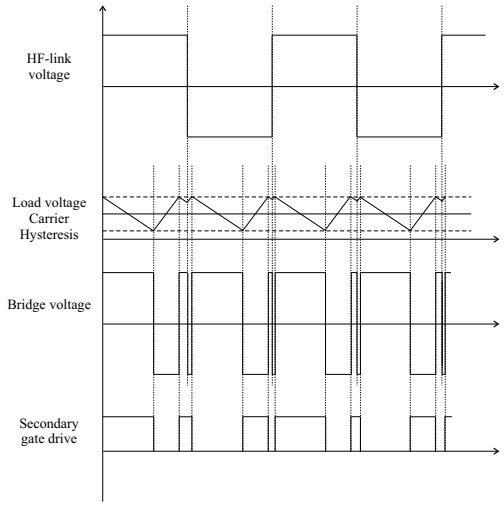

Fig. 4: Normal operation with $M < M^*_{lim}$

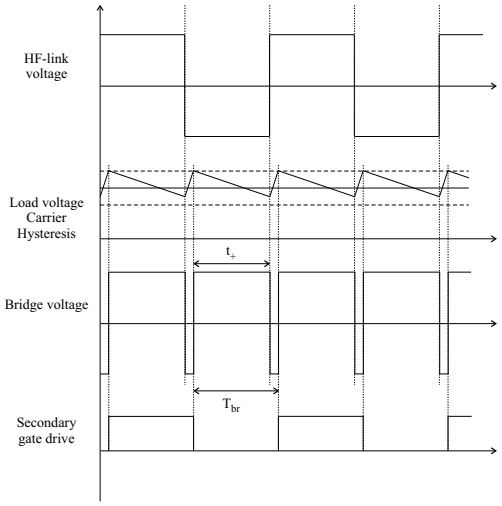

Fig. 5: Locked operation with $M \geq M^*_{lim}$

and MFB in Fig. 3 features attenuation equal to the gain of the SICAM amplifier k_a, leading to switching frequency of the output stage f_{s2} which is independent of the supply voltage V_s and significantly improving the PSRR:

$$f_{s2}(M) = f^*_{s2}(M) = \frac{1}{4}\frac{1-M^2}{\tau_{int}k_h k_a + t_d}\bigg|_{M<M^*_{lim}} \tag{4}$$

The idling switching frequency with $M = 0$ is:

$$f_{s2,0} = \frac{1}{4}\frac{1}{\tau_{int}k_h k_a + t_d} \tag{5}$$

4.4. Locked operation with $M \geq M^*_{lim}$

The real difference in the operation between the conventional self-oscillating modulator and the one for use with SICAMs is observed with modulation indexes larger than the modulation index limit $M \geq M^*_{lim}$. As shown in Fig. 5, the bridge voltage of the self-oscillating SICAMs with $M \geq M^*_{lim}$ turns into 2-level phase-shifted PWM with constant frequency two times the HF-link frequency:

$$f_{br} = 2 \cdot f_{s1} \tag{6}$$

while the output stage switching frequency is exactly equal to the input stage switching frequency i.e. the HF-link frequency:

$$f_{s2}(M) = f_{s1}\Big|_{M \geq M^*_{lim}} \tag{7}$$

With the duty cycle D defined as ratio between the time interval with high voltage on the bridge output t_+ and its period T_{br}, equal to half the HF-link period:

$$D = \frac{t_+}{T_{br}} = 2t_+ f_{s1} \tag{8}$$

the SICAM output voltage is calculated to be:

$$v_o = DV_s - (1-D)V_s = (2D-1)V_s \tag{9}$$

and the duty cycle dependance on the modulation index:

$$D = \frac{1 \pm M}{2} \tag{10}$$

where "+" sign is used for positive and "-" sign is used for negative reference voltages v_{ref}.

As implied in equations (6) and (7), the frequency of quantities associated with the secondary stage becomes locked to the primary side and the HF-link, since the slope of either the raising portion or the falling portion of the carrier has reduced as a result of the large modulation index $M \geq M^*_{lim}$. In this situation, the regular changes in the HF-link polarity interrupt the slower slope of one of the carrier portions before it hits the other wall of the hysteresis block, causing a sort of carrier reset. The time interval between the phase-shifted waveforms

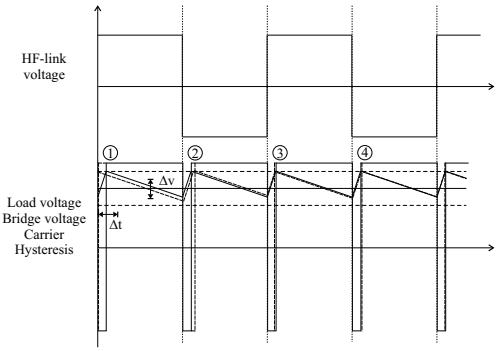

Fig. 6: Asymptotic stability of the locked operation

created by the switching of the output stage and the subsequent switching of the HF-link is essentially equal to the time interval with positive bridge voltage t_+ and its dependance on the modulation index is:

$$t_+ = DT_{br} = \frac{1 \pm M}{4 f_{s1}} \tag{11}$$

The phase locking property of the self-oscillating SICAM can be shown to be asymptotically stable. When disturbance voltage Δv is added to the carrier voltage, causing corresponding timing error Δt at the first switching of the output stage, like shown in Fig. 6, then the following equations for the subsequent errors are valid:

$$\begin{array}{lcllcl} \Delta t_1 & = & \Delta t & \Delta v_1 & = & \Delta v \\ \Delta t_2 & = & \left(\frac{1-M}{1+M}\right)\Delta t & \Delta v_2 & = & \left(\frac{1-M}{1+M}\right)\Delta v \\ \Delta t_3 & = & \left(\frac{1-M}{1+M}\right)^2\Delta t & \Delta v_3 & = & \left(\frac{1-M}{1+M}\right)^2\Delta v \\ \ldots & & & \ldots & & \\ \Delta t_{n+1} & = & \left(\frac{1-M}{1+M}\right)^n\Delta t & \Delta v_{n+1} & = & \left(\frac{1-M}{1+M}\right)^n\Delta v \end{array} \tag{12}$$

Because of the fact that:

$$\frac{1-M}{1+M} < 1 \tag{13}$$

the asymptotic stability of the timing interval t_+ for the phase-shifted PWM is proven:

$$\begin{array}{lcl} \Delta t_{n+1} & = & \left(\frac{1-M}{1+M}\right)^n \Delta t \xrightarrow{n\to\infty} 0 \\ \Delta v_{n+1} & = & \left(\frac{1-M}{1+M}\right)^n \Delta v \xrightarrow{n\to\infty} 0 \end{array} \tag{14}$$

With maximum modulation index M_{max}=1, the time interval t_+ of the phase shifted PWM approaches T_{br} and 0 with positive and negative voltages respectively, which means that at one instant close to the maximum modulation the switching of the input and output stage will start to overlap and the resultant bridge voltage will have switching frequency equal to the HF-link voltage $f_{br} = f_{s1} = f_{s2}$.

It is interesting to notice that, if the self-oscillating modulator is designed to have basic idling switching frequency lower than two times the HF-link frequency $f^*_{s2,0} < 2 \cdot f_{HF}$, i.e. $M^*_{lim} \equiv 0$, then the corresponding self-oscillating SICAM will be in locked operation all the time. Even more, if the maximum modulation index is limited to value less than one $M_{max} < 1$, then the switching of both stages is not simultaneous. This means that many other SICAM topologies which utilize safe-commutation strategies [2], [6] can be used in conjunction with the proposed self-oscillating modulator because of the natural synchronization between the stages during locked operation.

4.5. Output stage switching frequency

To summarize, the switching frequency of the output stage f_{s2} in the self-oscillating SICAM differs when operating in normal or locked mode and can be described with the following equation:

$$f_{s2} = \begin{cases} \dfrac{1}{4}\dfrac{1-M^2}{\tau_{int} k_h k_a + t_d} & , \quad M < M^*_{lim} \\ f_{s1} & , \quad M \geq M^*_{lim} \end{cases} \tag{15}$$

and represents a discontinuous function, shown in Fig. 7.

5. SICAM WITH ACTIVE CAPACITIVE VOLTAGE CLAMP

As mentioned earlier, the load current commutation in the self-oscillating SICAMs can be most reliably performed by using clamps, which clamp the load and output filter voltage to the clamp capacitor voltage and provide current path during the dead or blanking time t_{bl} between the outgoing and incoming switches. The active clamping technology [7] where the clamped energy is returned to the primary side via an auxiliary small power converter is regarded as superior to the dissipative one [4], because of the much higher efficiency, but on expense of few additional components, handling just

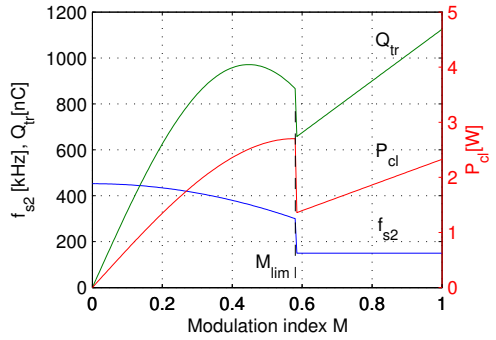

Fig. 7: Output stage switching frequency, transferred charge and clamp power

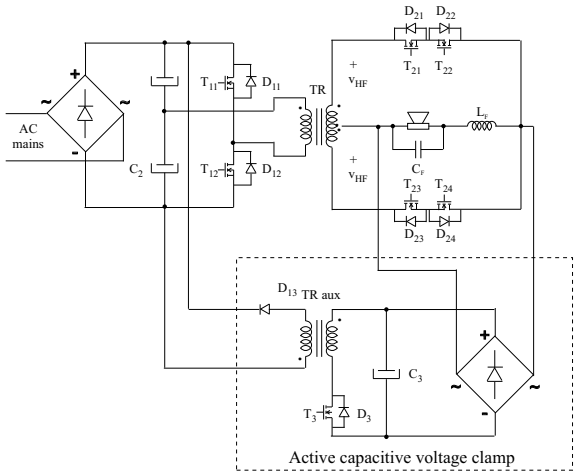

Fig. 8: SICAM with active capacitive voltage clamp

a small fraction of the output power. The scheme of the SICAM with active capacitive voltage clamp is given in Fig. 8.

The voltage of the clamp capacitor is regulated by feedback to a value slightly higher than the HF-link voltage $V_{cl} > V_s$, so that the clamp is charged only during the blanking time intervals. The auxiliary converter can be made in many different topologies, with the flyback converter as simplest choice.

The design of the clamp starts with the selection of the clamp capacitor $C_{cl} \equiv C_3$ in Fig. 8. The primary task of the selection process is to limit the voltage ripple ΔV_{cl} during normal operation or emergency shutdown. By assuming that the bulk of the clamp capacitor voltage ripple in normal operation is due to its internal equivalent series resistance (ESR), the following selection rule can be written for the clamp capacitor ESR:

$$ESR_{max} = \frac{\Delta V_{cl,max}}{I_{o,max}} \tag{16}$$

where $\Delta V_{cl,max}$ is the maximum voltage ripple during normal operation and $I_{o,max}$ is the peak output current.

During emergency shutdown all the stored energy in the output filter inductor is converted into electrostatic energy in the clamp capacitor. By neglecting the presence of the auxiliary converter due to the unavoidable time delay before it catches up with the increased clamp voltage, the clamp capacitor capacitance is limited to:

$$C_{cl,min} = L_f \left(\frac{I_{o,max}}{\Delta V_{cl,max}} \right)^2 \tag{17}$$

where L_f is the output filter inductance and $\Delta V_{cl,max}$ refers to the maximum allowed voltage excursion in a case of emergency shutdown.

In the same time, the clamp capacitor must be able to handle the maximum RMS clamp current during normal operation:

$$I_{cl,rms,max} = \frac{2}{\pi} I_{o,max} \sqrt{D} = \frac{2}{\pi} I_{o,max} \sqrt{t_{bl} f_{s2}} \tag{18}$$

The most important quantity for the design of the auxiliary converter is the maximum transferred charge $Q_{tr,max}$ from the load to the clamp during one period of the auxiliary converter operation $T_{aux} = 1/f_{aux}$, assuming that the latter is able to return that charge to the primary side and regain the balance on the clamp capacitor voltage. Due to the discontinuity of the output stage switching frequency function in (15), normal and locked operation must be dealt separately:

- normal operation

$$\begin{aligned} Q_{tr,n} &= \frac{f_{s2,0}}{f_{aux}} (1 - M^2) M I_{o,max} t_{bl} \\ \left. \frac{dQ_{tr,n}}{dM} \right|_{M=M_n} &= \frac{f_{s2,0}}{f_{aux}} I_{o,max} t_{bl} (1 - 3M^2) = 0 \\ M_n &= \frac{1}{\sqrt{3}} \text{ if } M_n < M_{lim} \\ Q_{tr,max,n} &= \frac{2}{3\sqrt{3}} \frac{f_{s2,0}}{f_{aux}} I_{o,max} t_{bl} \end{aligned} \tag{19}$$

- locked operation

$$\begin{aligned} Q_{tr,l} &= \frac{f_{s1}}{f_{aux}} M I_{o,max} t_{bl} \\ \left.\frac{dQ_{tr,l}}{dM}\right|_{M=M_l} &= 0 \\ M_l &= M_{max} \\ Q_{tr,max,l} &= \frac{f_{s1}}{f_{aux}} M_{max} I_{o,max} t_{bl} \end{aligned} \tag{20}$$

Finally, the maximum transferred charge during one switching period of the auxiliary converter is:

$$Q_{tr,max} = \max\{Q_{tr,max,n}, Q_{tr,max,l}\} \tag{21}$$

The charge transferred to the clamp Q_{tr} is depicted in Fig. 7.

Power handled by the auxiliary converter P_{cl}, shown also in Fig. 7, is calculated as:

$$P_{cl} = V_{cl} I_{cl,av} = V_{cl} t_{bl} f_{s2} \frac{2}{\pi} M I_{o,max} \tag{22}$$

and the clamp power loss is just a fraction of P_{cl}:

$$P_{loss,cl} = \eta(P_{cl}) \cdot P_{cl} \tag{23}$$

5.1. Audio distortion

The distortion mechanism in the SICAM with active capacitive voltage clamp is very similar to the one in the conventional Class D amplifiers [15]. The only difference is that during the blanking time periods t_{bl} the load voltage is equal to the clamp capacitor voltage V_{cl} and the average voltage error v_e, shown in Fig. 9 is:

$$v_e = \begin{cases} -\dfrac{2t_{bl}V_{cl}}{T_{s2}} & , \quad i_0 > 0 \\ \dfrac{2t_{bl}V_{cl}}{T_{s2}} & , \quad i_0 < 0 \end{cases} \tag{24}$$

The Fourier coefficients of the voltage error in (24) are given by the following equations:

$$\begin{aligned} a_0 &= 0 \\ a_n &= 0 \\ b_n &= -2\frac{t_{bl}}{T_{s2}} V_{cl} \frac{sin(n\frac{\pi}{2})}{n\frac{\pi}{2}} = 2\frac{t_{bl}}{T_{s2}} V_{cl} \frac{(-1)^n}{(2n-1)\frac{\pi}{2}} \end{aligned} \tag{25}$$

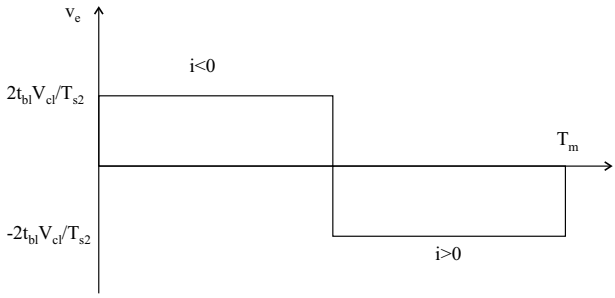

Fig. 9: Average voltage error v_e of the SICAM with active capacitive voltage clamp

and the Total Harmonic Distortion (THD) of the "conditionally" open-loop SICAM power stage with active capacitive voltage clamp is:

$$THD = \frac{\sqrt{\sum_{i=2}^{N_{max}} b_i^2}}{MV_s - \frac{4t_{bl}V_{cl}}{\pi T_{s2}}} \tag{26}$$

The notion "conditionally" means that the THD is calculated for the power stage without any additional correction from feedback loops, although it is obvious that the self-oscillating SICAM cannot operate without the MFB.

The presence of filter ripple current causes the THD of the SICAM to decrease as the output current i.e. the modulation index M decreases. This is result of the fact that within one switching period T_{s2} the switch current changes the polarity, thus effectively cancelling the voltage error of two subsequent load current commutations and giving no average voltage error. Therefore, the reduced THD of the SICAM at low modulation indexes can be taken into account the same way as in the conventional Class D amplifier [15]. THD of the SICAM with active capacitive voltage clamp in "conditionally" open loop with modulation signal of $f_m = 1$ kHz is shown in Fig. 10. THD gradually decreases with higher modulation indexes as the result of the falling switching frequency and the increased switching period T_{s2}, while the blanking time t_{bl} stays essentially the same.

6. INTEGRATED MAGNETICS FOR SICAM WITH ACTIVE CLAMP

Although the proposed SICAM with active capacitive voltage clamp has much higher efficiency due to the recycling of the dumped clamp energy, it is by no means

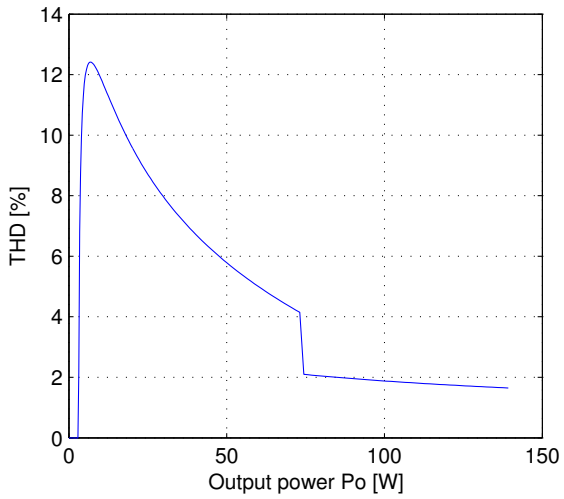

Fig. 10: THD of SICAM with active capacitive voltage clamp

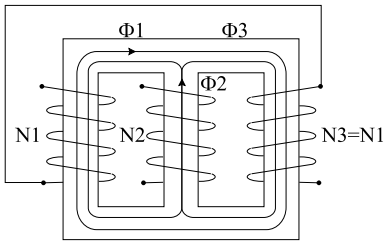

Fig. 11: Integrated magnetics

as simple and cost effective as the dissipative clamp solutions [4]. One way to reduce the complexity of the active clamp and reduce component count is to introduce special integrated magnetics, which incorporates the auxiliary transformer on the same magnetic core with the main power transformer. The principal approach is shown in Fig. 11, where the main transformer winding N_2 creates flux Φ_2 in the center leg and outer windings, which is independent of the flux $\Phi_1 = \Phi_3$ flowing entirely in the outer legs, caused by the magnetomotive forces of the serially connected and identical windings N_1 and N_3. In this way, the magnetic structure associated with the central leg and winding N_2 is totally independent from the magnetic structure associated with the windings N_1 and N_3 on the outer legs.

One particular implementation of the proposed integrated magnetics for the SICAM with active capacitive voltage clamp, where the auxiliary transformer uses the outer legs, is shown in Fig. 12.

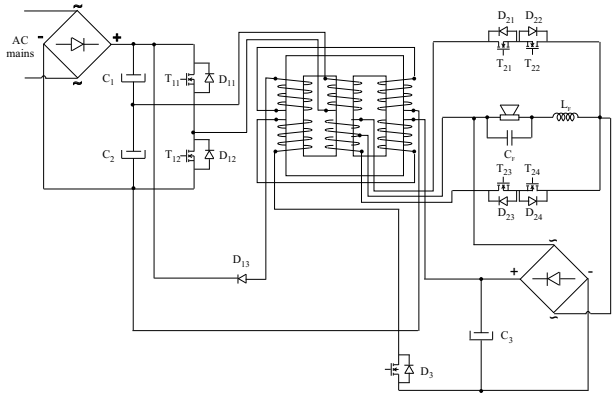

Fig. 12: Integrated magnetics for the SICAM with active clamp

7. SIMULATION RESULTS

In order to test the feasibility of the proposed self-oscillating modulators for SICAMs, series of PSpice simulations were performed. The simulated SICAM prototype with output power of 100W @ 8Ω features free-running input stage at $f_{s1} = 150$ kHz and single-ended secondary-side bidirectional bridge with $f_{s2,0} \approx 450$ kHz. It runs a modified GLIM modulator, as shown in Fig. 3.

The simulated waveforms of the output voltage, carrier voltage, bridge voltage and HF-link voltage of a GLIM self-oscillating SICAM are presented in Fig. 13 and the FFT of the output voltage is shown in Fig. 14, with $M = 0.75$ and 10 kHz reference. Both the normal operation mode with lower modulation indexes and the locked operation mode with larger modulation indexes are clearly visible. Normal operation mode with $M = 0.25 < M_{lim}$ DC reference and locked operation mode with $M = 0.75 > M_{lim}$ DC reference featuring phase-shifted PWM bridge voltage are shown in Fig. 15 and Fig. 16, which appear the same as in the theoretical investigation.

8. CONCLUSION

This paper presented how common self-oscillating modulators intended for use in Class D amplifiers can be

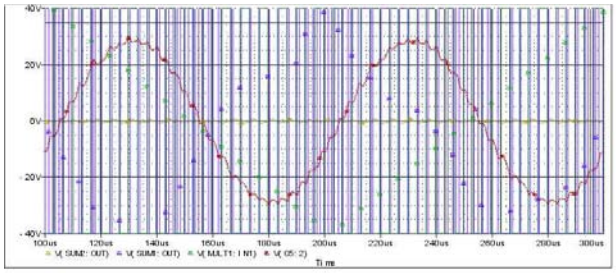

Fig. 13: Output voltage, carrier voltage, bridge voltage and HF-link voltage with $M = 0.75$ and 10 kHz reference

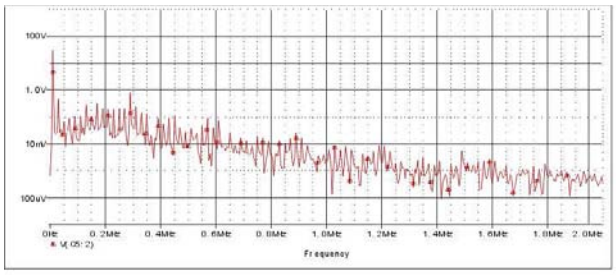

Fig. 14: FFT of the output voltage with $M = 0.75$ and 10 kHz reference

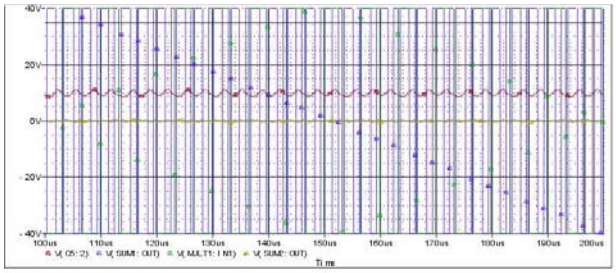

Fig. 15: Output voltage, carrier voltage, bridge voltage and HF-link voltage in normal operation mode with $M = 0.25 < M_{lim}$ DC reference

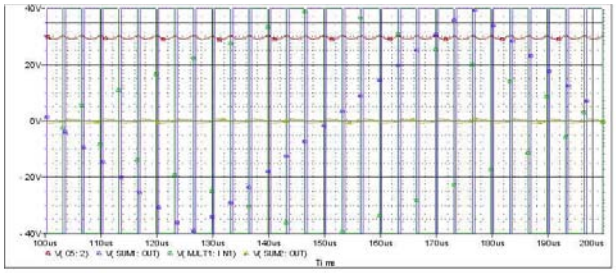

Fig. 16: Output voltage, carrier voltage, bridge voltage and HF-link voltage in locked operation mode with $M = 0.75 > M_{lim}$ DC reference

modified for implementation in direct energy conversion audio power amplifiers i.e. SICAMs. Although the modification was realized on a GLIM type self-oscillating modulator, results are general and widely applicable. In principle, two similar self-oscillating modulators, one for the positive polarity and one for the negative polarity of the HF-link are operating in parallel and the corresponding output is chosen based on the instantaneous HF-link voltage polarity. Two distinct modes of operation, namely the normal variable frequency mode and the locked constant frequency mode have been identified and thoroughly analyzed. The audio distortion of the self-oscillating SICAM with an active capacitive voltage clamp for easy load current commutation has been found to have similar form to the conventional Class D amplifier. Integrated magnetics has been described, which incorporates both the main and the auxiliary transformer on the same magnetic core. Finally, simulated waveforms of a prototype were presented and showed the viability of the approach.

ACKNOWLEDGMENT

The SICAM project is funded under the grant of the Danish Energy Authority EFP no. 1273/02-0001 and is performed in cooperation with Bang & Olufsen ICEpower a/s in Kgs. Lyngby, Denmark.

9. REFERENCES

[1] P. Ljušev and M. Andersen, “Approaches to building single-stage ac/ac conversion switch-mode audio power amplifiers,” in *Proc. 11th International Power Electronics and Motion Control conference EPE-PEMC 2004*, (Riga, Latvia), September 2-4 2004.

[2] P. Ljušev and M. Andersen, "Switching-mode audio power amplifiers with direct energy conversion," in *118th AES Convention*, (Barcelona, Spain), May 28-31 2005.

[3] D. Mitchell, "Dc to low frequency inverter with pulse width modulated high frequency link," *U.S. patent 4,339,791*, July 1982.

[4] B. E. Attwood, L. E. Hand, and L. C. Santillano, "Audio amplifier with phase modulated pulse width modulation," *U.S. patent 4,992,751*, February 1991.

[5] K. Nielsen and L. M. Fenger, "The active pulse modulated transducer (at) a novel audio power conversion system architecture," in *115th Convention of the Audio Engineering Society, AES Proceedings*, October 10-13 2003. Preprint 5866.

[6] P. Ljušev and M. Andersen, "Safe-commutation principle for direct single-phase ac-ac converters for use in audio power amplification," in *Proc. Nordic Workshop on Power and Industrial Electronics NORPIE 2004*, (Trondheim, Norway), June 14-16 2004.

[7] P. Ljušev and M. Andersen, "Direct-conversion switching-mode audio power amplifier with active capacitive voltage clamp," in *36th IEEE Power Electronics Specialists Conference PESC 2005*, (Recife, Brazil), June 12-16 2005.

[8] P. Espelage and B. Bose, "High-frequency link power conversion," *IEEE Transactions on Industry Applications*, vol. IA-13, no. 5, pp. 387–94, 1977.

[9] S. Poulsen and M. Andersen, "Self oscillating pwm modulators a topological comparison," in *Proc. IEEE Power Modulators conference PMC 2004*, (San Francisco, USA), 2004.

[10] T. Frederiksen, H. Bengtsson, and K. Nielsen, "A novel audio power amplifier topology with high efficiency and state-of-the-art performance," in *109th Convention of the Audio Engineering Society, AES Proceedings*, September 22-25 2003. Preprint 5197.

[11] P. van der Hulst, A. Veltman, and R. Groenenberg, "An asynchronous switching high-end amplifier," in *112th Convention of the Audio Engineering Society, AES Proceedings*, May 10-13 2002. Preprint 5503.

[12] S. Poulsen, *Towards active transducers*. PhD thesis, Technical University of Denmark, Kgs. Lyngby, Denmark, July 2004.

[13] "Selbstschwingender digitalverstärker," *German patent DE 19838765 A1, ELBO GmbH*, May 2000.

[14] S. Poulsen and M. Andersen, "Simple pwm modulator with excellent dynamic behavior," in *Applied Power Electronics Conference APEC 2004*, (Anaheim, USA), 2004.

[15] K. Nielsen, "Linearity and efficiency performance of switching audio power amplifier output stage - a fundamental analysis," in *105th Convention of the Audio Engineering Society, AES Proceedings*, September 26-29 1998. Preprint 4838 (E-4).